

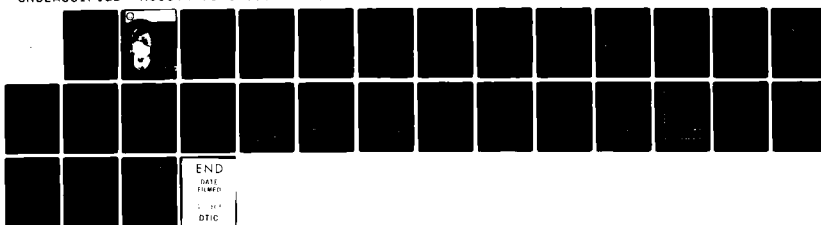
AD-A126 302

A PHASE CORRECTION FILTER FOR WAVEFORM RECOVERY OF
COMPRESSED DIRECT-RECO..(U) WASHINGTON UNIV SEATTLE
DEPT OF OCEANOGRAPHY U S WADE ET AL. MAR 81 REF-M81-05
UNCLASSIFIED N00014-75-C-0502

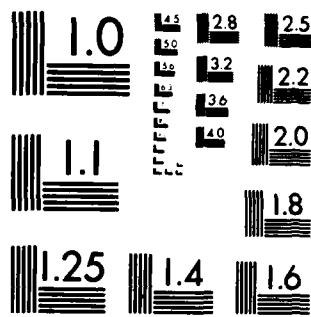
1/1

F/G 8/10

NL



END
DATE
FILED
L M A
DTIC



MICROCOPY RESOLUTION TEST CHART
NATIONAL BUREAU OF STANDARDS-1963-A



the department of
OCEANOGRAPHY

12

ADA126302



DTIC FILE COPY

This document has been approved
for public release and sale; its
distribution is unlimited.

TECHNICAL REPORT NO. 385

A PHASE CORRECTION FILTER
FOR WAVEFORM RECOVERY OF
COMPRESSED DIRECT-RECORDED
OCEAN BOTTOM SEISMOMETER DATA

by

Ules S. Wade
Clive R.B. Lister

Office of Naval Research
Contract N-00014-75-C-0502
MOD P00021
Project NR 083-012

Reference M81-05
March 1981

DTIC
ELECTE
APR 4 1983

A

seattle, washington 98195
83 04 01 020

UNIVERSITY OF WASHINGTON
DEPARTMENT OF OCEANOGRAPHY
Seattle, Washington 98195

Technical Report No. 385

A phase correction filter for waveform recovery of compressed
direct-recorded ocean bottom seismometer data.

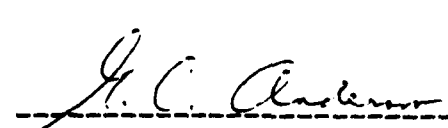
by

Ules S. Wade
Clive R.B. Lister

Office of Naval Research
Contract N-00014-75-C-0502 MOD P00021
Project NR 083-012


C. R. B. Lister
Principal Investigator

Reference MB1-05
March 1981


George Anderson
Associate Chairman for Research

Reproduction in whole or in part is permitted
for any purpose of the United States government

ABSTRACT

A phase convolution filter has been developed for the University of Washington's ocean bottom seismometers (OBS) to correct severe waveform distortion on playback. Signals are recorded directly on magnetic tape after compression by taking the bipolar square-root of the signal. Prior to digitization, the analog playback head shifts the phases of the low frequency harmonics and thus distorts the recorded waveform. If the distorted signal is squared without correction, the original waveforms and bandwidths are not recovered, leading to errors in the selection of arrival times and an inability to analyse the seismic coda for late arrivals. The phase-correcting filter has been constructed by inverting a smoothed version of the spike spectrum that results when a square wave is recorded on the tape.

1		Accession For	<input checked="" type="checkbox"/>	
2		THIS GRA&I	<input type="checkbox"/>	
3		EXIC TAB	<input type="checkbox"/>	
4		W-Indemnized	<input type="checkbox"/>	
5		Justification	<input type="checkbox"/>	
6		S-1000		
7		S-1000		
8		S-1000		
9		S-1000		
10		S-1000		
11		S-1000		
12		S-1000		
13		S-1000		
14		S-1000		
15		S-1000		
16		S-1000		
17		S-1000		
18		S-1000		
19		S-1000		
20		S-1000		
21		S-1000		
22		S-1000		
23		S-1000		
24		S-1000		
25		S-1000		
26		S-1000		
27		S-1000		
28		S-1000		
29		S-1000		
30		S-1000		
31		S-1000		
32		S-1000		
33		S-1000		
34		S-1000		
35		S-1000		
36		S-1000		
37		S-1000		
38		S-1000		
39		S-1000		
40		S-1000		
41		S-1000		
42		S-1000		
43		S-1000		
44		S-1000		
45		S-1000		
46		S-1000		
47		S-1000		
48		S-1000		
49		S-1000		
50		S-1000		
51		S-1000		
52		S-1000		
53		S-1000		
54		S-1000		
55		S-1000		
56		S-1000		
57		S-1000		
58		S-1000		
59		S-1000		
60		S-1000		
61		S-1000		
62		S-1000		
63		S-1000		
64		S-1000		
65		S-1000		
66		S-1000		
67		S-1000		
68		S-1000		
69		S-1000		
70		S-1000		
71		S-1000		
72		S-1000		
73		S-1000		
74		S-1000		
75		S-1000		
76		S-1000		
77		S-1000		
78		S-1000		
79		S-1000		
80		S-1000		
81		S-1000		
82		S-1000		
83		S-1000		
84		S-1000		
85		S-1000		
86		S-1000		
87		S-1000		
88		S-1000		
89		S-1000		
90		S-1000		
91		S-1000		
92		S-1000		
93		S-1000		
94		S-1000		
95		S-1000		
96		S-1000		
97		S-1000		
98		S-1000		
99		S-1000		
100		S-1000		
101		S-1000		
102		S-1000		
103		S-1000		
104		S-1000		
105		S-1000		
106		S-1000		
107		S-1000		
108		S-1000		
109		S-1000		
110		S-1000		
111		S-1000		
112		S-1000		
113		S-1000		
114		S-1000		
115		S-1000		
116		S-1000		
117		S-1000		
118		S-1000		
119		S-1000		
120		S-1000		
121		S-1000		
122		S-1000		
123		S-1000		
124		S-1000		
125		S-1000		
126		S-1000		
127		S-1000		
128		S-1000		
129		S-1000		
130		S-1000		
131		S-1000		
132		S-1000		
133		S-1000		
134		S-1000		
135		S-1000		
136		S-1000		
137		S-1000		
138		S-1000		
139		S-1000		
140		S-1000		
141		S-1000		
142		S-1000		
143		S-1000		
144		S-1000		
145		S-1000		
146		S-1000		
147		S-1000		
148		S-1000		
149		S-1000		
150		S-1000		
151		S-1000		
152		S-1000		
153		S-1000		
154		S-1000		
155		S-1000		
156		S-1000		
157		S-1000		
158		S-1000		
159		S-1000		
160		S-1000		
161		S-1000		
162		S-1000		
163		S-1000		
164		S-1000		
165		S-1000		
166		S-1000		
167		S-1000		
168		S-1000		
169		S-1000		
170		S-1000		
171		S-1000		
172		S-1000		
173		S-1000		
174		S-1000		
175		S-1000		
176		S-1000		
177		S-1000		
178		S-1000		
179		S-1000		
180		S-1000		
181		S-1000		
182		S-1000		
183		S-1000		
184		S-1000		
185		S-1000		
186		S-1000		
187		S-1000		
188		S-1000		
189		S-1000		
190		S-1000		
191		S-1000		
192		S-1000		
193		S-1000		
194		S-1000		
195		S-1000		
196		S-1000		
197		S-1000		
198		S-1000		
199		S-1000		
200		S-1000		
201		S-1000		
202		S-1000		
203		S-1000		
204		S-1000		
205		S-1000		
206		S-1000		
207		S-1000		
208		S-1000		
209		S-1000		
210		S-1000		
211		S-1000		
212		S-1000		
213		S-1000		
214		S-1000		
215		S-1000		
216		S-1000		
217		S-1000		
218		S-1000		
219		S-1000		
220		S-1000		
221		S-1000		
222		S-1000		
223		S-1000		
224		S-1000		
225		S-1000		
226		S-1000		
227		S-1000		
228		S-1000		
229		S-1000		
230		S-1000		
231		S-1000		
232		S-1000		
233		S-1000		
234		S-1000		
235		S-1000		
236		S-1000		
237		S-1000		
238		S-1000		
239		S-1000		
240		S-1000		
241		S-1000		
242		S-1000		
243		S-1000		
244		S-1000		
245		S-1000		
246		S-1000		
247		S-1000		
248		S-1000		
249		S-1000		
250		S-1000		
251		S-1000		
252		S-1000		
253		S-1000		
254		S-1000		
255		S-1000		
256		S-1000		
257		S-1000		
258		S-1000		
259		S-1000		
260		S-1000		
261		S-1000		
262		S-1000		
263		S-1000		
264		S-1000		
265		S-1000		
266		S-1000		
267		S-1000		
268		S-1000		
269		S-1000		
270		S-1000		
271		S-1000		
272		S-1000		
273		S-1000		
274		S-1000		
275		S-1000		
276		S-1000		
277		S-1000		
278		S-1000		
279		S-1000		
280		S-1000		
281		S-1000		
282		S-1000		
283		S-1000		
284		S-1000		
285		S-1000		
286		S-1000		
287		S-1000		
288		S-1000		
289		S-1000		
290		S-1000		
291		S-1000		
292		S-1000		
293		S-1000		
294		S-1000		
295		S-1000		
296		S-1000		
297		S-1000		
298		S-1000		
299		S-1000		
300		S-1000		
301		S-1000		
302		S-1000		
303		S-1000		
304		S-1000		
305		S-1000		
306		S-1000		
307		S-1000		
308		S-1000		
309		S-1000		
310		S-1000		
311		S-1000		
312		S-1000		
313		S-1000		
314		S-1000		
315		S-1000		
316		S-1000		
317		S-1000		
318		S-1000		
319		S-1000		
320		S-1000		
321		S-1000		
322		S-1000		
323		S-1000		
324		S-1000		
325		S-1000		
326		S-1000		
327		S-1000		
328		S-1000		
329		S-1000		
330		S-1000		
331		S-1000		
332		S-1000		
333		S-1000		
334		S-1000		
335		S-1000		
336		S-1000		
337		S-1000		
338		S-1000		
339		S-1000		
340		S-1000		
341		S-1000		
342		S-1000		
343		S-1000		
344		S-1000		
345		S-1000		
346		S-1000		
347		S-1000		
348		S-1000		
349		S-1000		
350		S-1000		
351		S-1000		
352		S-1000		
353		S-1000		
354		S-1000		
355		S-1000		
356		S-1000		
357		S-1000		
358		S-1000		
359		S-1000		
360		S-1000		
361		S-1000		
362		S-1000		
363		S-1000		
364		S-1000		
365		S-1000		
366		S-1000		
367		S-1000		
368		S-1000		
369		S-1000		
370		S-1000		
371		S-1000		
372		S-1000		
373		S-1000		
374		S-1000		
375		S-1000		
376		S-1000		
377		S-1000		
378		S-1000		
379		S-1000		
380		S-1000		
381		S-1000		
382		S-1000		
383		S-1000		
384		S-1000		
385		S-1000		
386		S-1000		
387		S-1000		
388		S-1000		
389		S-1000		
390		S-1000		
391		S-1000		
392		S-1000		
393		S-1000		
394		S-1000		
395		S-1000		
396		S-1000		
397		S-1000		
398		S-1000		
399		S-1000		
400		S-1000		
401		S-1000		
402		S-1000		
403		S-1000		
404		S-1000		
405		S-1000		
406		S-1000		
407		S-1000		
408		S-1000		
409		S-1000		
410		S-1000		
411		S-1000		
412		S-1000		
413		S-1000		
414		S-1000		

ACKNOWLEDGEMENTS

We would like to thank Rex Johnson, Brian Lewis, and the officers and crew of the Thomas G. Thompson for aid in successfully gathering the data used in this analysis.

Financial support was provided by the Office of Naval Research under contracts N-00014-67-A-0103-0014 and N-00014-75-C-0502 MOD PU0021.

TABLE OF CONTENTS

	Page
ABSTRACT.....	iii
ACKNOWLEDGEMENTS.....	iv
LIST OF FIGURES.....	vi
INTRODUCTION.....	1
FILTER DESIGN.....	2
PROPERTIES OF FOURIER TRANSFORM PAIRS.....	7
EXPERIMENTAL PROCEDURE.....	8
COMPUTATION OF THE FILTER.....	8
TIME DOMAIN REPRESENTATION OF THE FILTER.....	15
RESULTS.....	15
CONCLUSIONS.....	19
REFERENCES.....	21

LIST OF FIGURES

	Page
1. Frequency response of the OBS electronics.....	3
2. Transfer function of the OBS electronics.....	4
3. Five hertz calibration sine wave.....	5
4. Square wave output.....	6
5. Imaginary part of the complex inverse filter.....	11
6. Real part of the complex inverse filter.....	12
7. Spectra of square wave and distorted output.....	13
8. Phase response of square wave, distorted output, and inverse filter.....	14
9. Amplitude spectra of the inverse phase filter.....	16
10. Distorted square wave after inverse filtering.....	17
11. Seismic signal after processing.....	18

INTRODUCTION

Ocean bottom seismometers have been used in marine geophysical investigations to eliminate the shortcomings of free floating surface receivers. The University of Washington's OBS as described by Lister and Lewis, 1976, was designed with simplicity as the primary goal and has had a very high recovery rate both for the instruments and for usable data (Johnson et al. 1977). We will describe here only those features of the OBS pertinent to the solution of the waveform fidelity problem that arose when the direct-recorded data tapes were played back into a digitizer.

Three orthogonal components of motion are measured using L 15 B Mark Products 4.5 hertz geophones. They are leveled in a boat floating on silicone oil of a thickness chosen to place the high pass filter corner frequency well below 0.5 hertz. The signal from the sensors is amplified and passed through two three-pole Bessel filters to define a 2 to 100 hertz passband with a minimum of time-envelope distortion. The filtering limits the signal to within the band pass capabilities of the tape recorder. Dynamic-range compression is accomplished by taking the square root of the signal deviation, negative values being handled by a separate circuit, and the results recombined with sign preservation. Square-rooting generates low harmonic and cross-modulation distortion, consistent with substantial compression, and does not require a calibration level, since the transition to linear response can be made low enough to vanish in the background noise level. The harmonic content of a square-rooted sine wave is about 26 percent, and is independent of amplitude. The signal is recorded by a slow speed direct method on tape moving at 1mm per second, together with a clock signal encoded with the day, hour, minute, and second. On playback, a mini-computer is used to digitize all four channels and decode the clock in software. The analog tapes are played back on a slightly modified Hewlett-Packard 3960 series tape recorder, at a speed approximately 25 times the recording speed. A four-pole 20 hertz notch filter is used to eliminate the noise induced by vibration of the OBS tape drive motor. The signal is amplified by a tracking three-channel buffer amplifier until the largest signal peaks approach the limits of the digitizer's range. The sample spacing is 0.01 seconds in OBS time, or 2500 samples per second at playback speed, so that a 1250 hertz low-pass Butterworth filter could be inserted in the analog signal processing chain to reduce

aliasing.

In figure 1, the measured frequency response of the electronic package (filled circles) is compared to the calculated response (open circles) of the electronics plus geophone sensor (Lee Bond, unpublished technical report). A 2 volt signal was inserted at the calibration input, attenuated by 1000, and then measured at the record head to produce the solid line in figure 1. The theoretical response of the geophone was calculated from the manufacturer's specifications and combined with the calculated response of the electronics. The combined response is minus 3db in amplitude at 4.5 hertz, but is essentially flat from 8 to 50 hertz. The square root circuitry was calibrated in a cold room to verify that it follows the proper power law. This data (figure 2) produced the regression relationship $VOLTS_{out} = \text{SQRT}(K * VOLTS_{in})$ for an input voltage of 10 millivolts to 10 volts. The constant factor, K, is 4.5.

A 5 hertz calibration signal was recorded on the OBS, digitized, and squared to show the type of waveform distortion generated by the analog playback head (figure 3). In addition, the digitized output of a perfect 2 hertz square wave (figure 4) demonstrates that the lowest harmonic has been phase shifted but the higher harmonics which combine to preserve the sharp onset, have not.

FILTER DESIGN

A filter can be realized by comparison of a distorted output with the original undistorted signal, in frequency space, simply by the division of the latter by the former. The frequency domain filter can then be inverted to a time domain filter, and applied to the signal by convolution to avoid the windowing problems of finite discrete transforms. When constructing this type of filter, it is helpful to have the discrete frequencies of the Fourier transform matched to the harmonics present in the test signal. This criterion avoids the need for vectorial addition of the Fourier frequencies near the test wave frequencies, and is satisfied by having a whole number of test wave cycles in the transform time window.

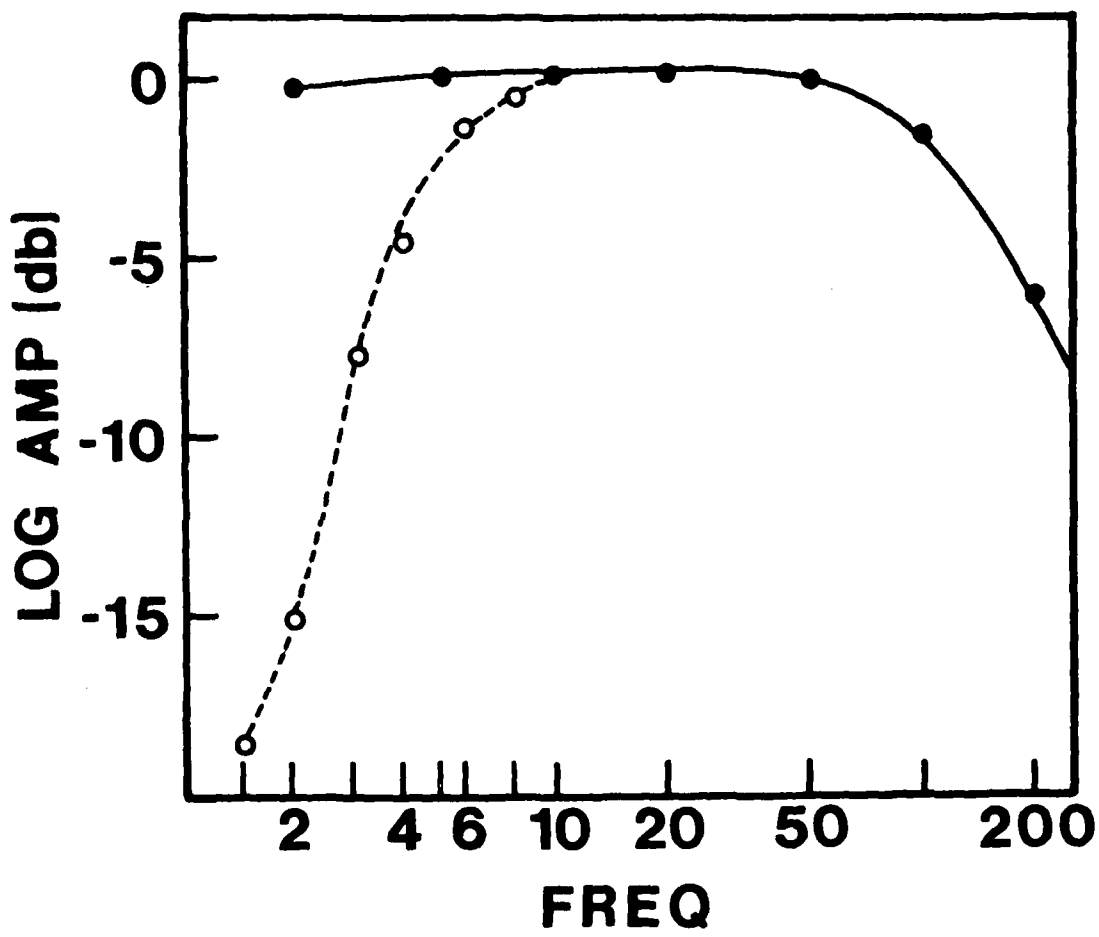


FIGURE 1. Measured frequency response of the OBS. The solid line is the response of the electronics. The dashed line is the calculated response of the electronics including the geophone sensor. Redrawn from L. Bond, unpublished technical report 1979.

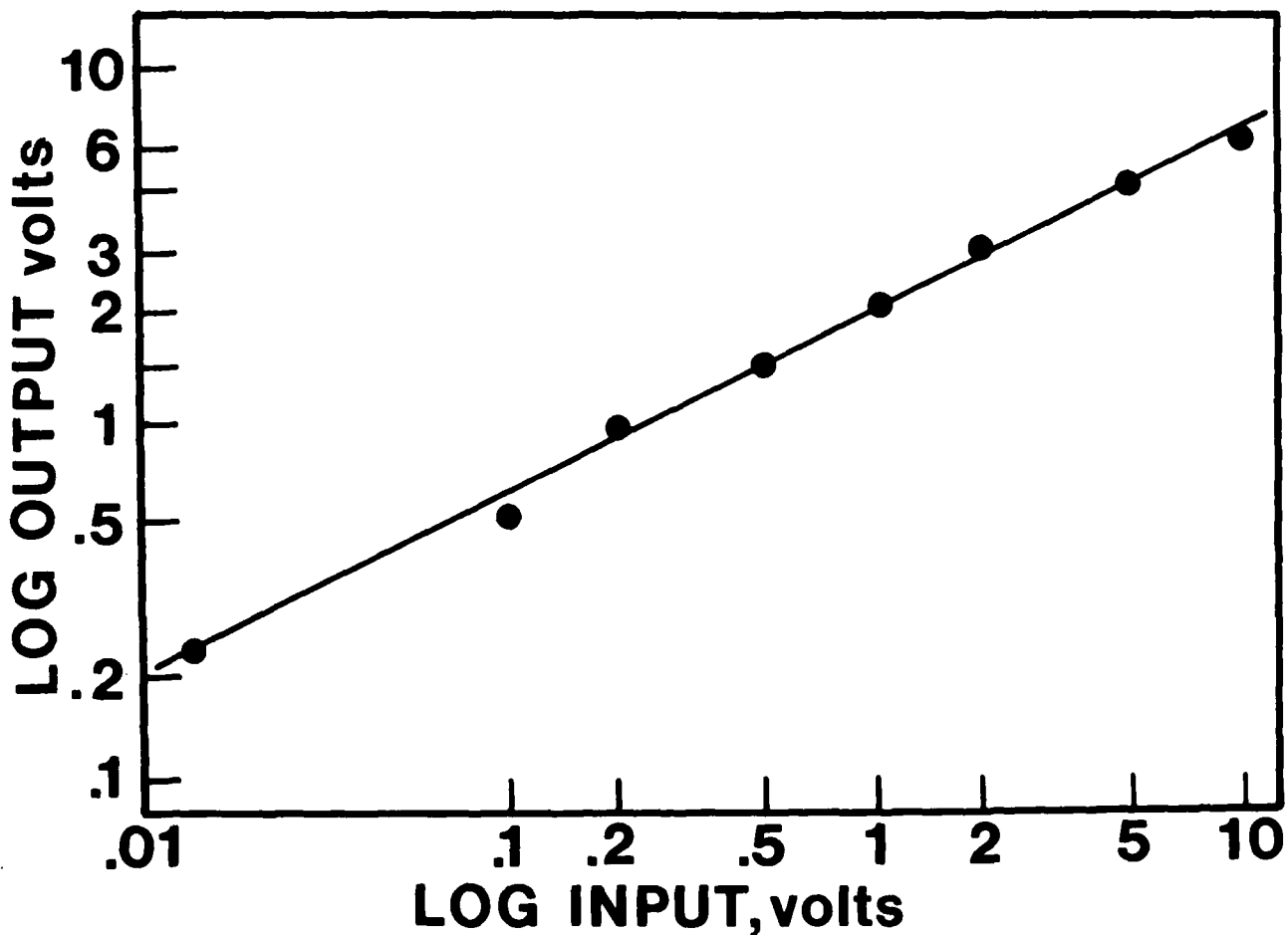


FIGURE 2. Measured transfer function of the OBS electronics including square-root circuitry. The data was taken at 5 hertz. Redrawn from L. Bond, unpublished technical report 1979.

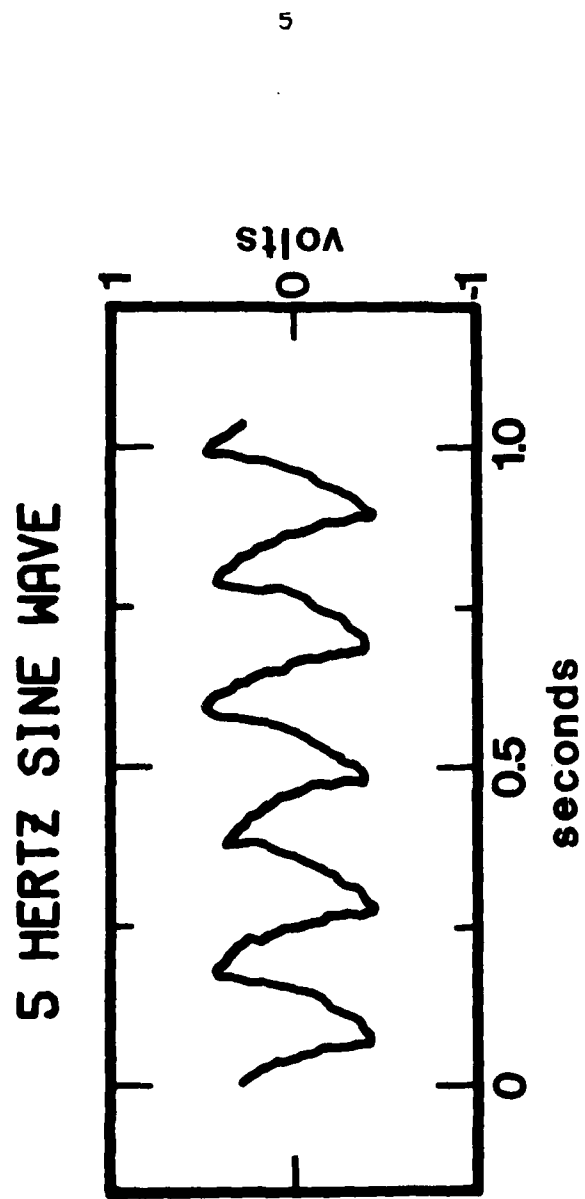


FIGURE 3. The digitized output of a 5 hertz calibration sine wave. Note scalloped waveform.

OUTPUT OF 2 HERTZ SQUARE WAVE

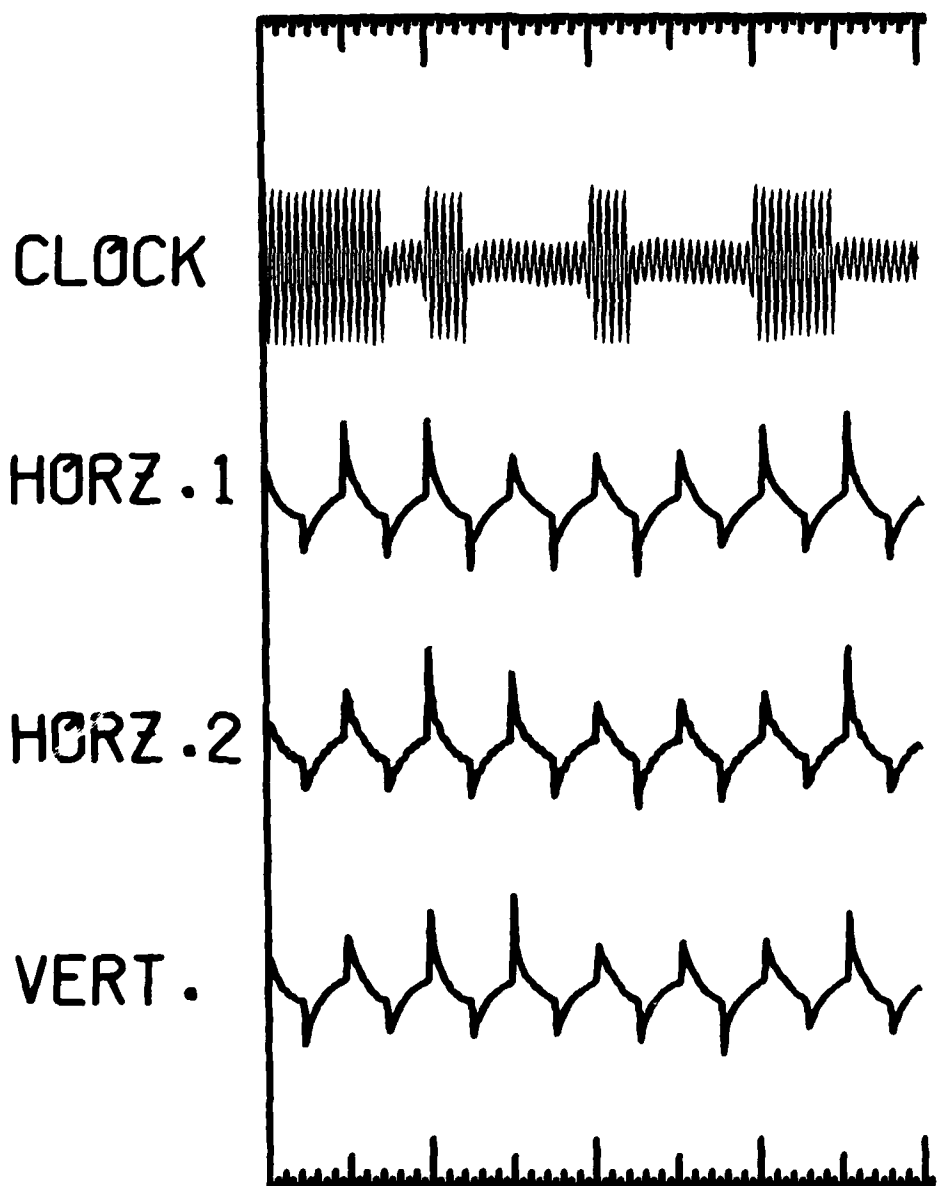


FIGURE 4. The digitized output of an inputted square wave.
The identical signal was fed into all 3 channels.

PROPERTIES OF FOURIER TRANSFORM PAIRS

The Fourier pairs $f(t)$ and $F(\omega)$ have properties that simplify computation in the frequency domain. A physically realizable time function, i.e. any geophysical record, is a pure real function, and the corresponding $F(\omega)$ is complex and is defined for both positive and negative ω up to the Nyquist frequency. Thus it contains redundant information, described by

$$F(\pm\omega) = F^*(\mp\omega)$$

This implies that the real part of $F(\omega)$ is even (the same for positive and negative ω) and the imaginary part is odd. A function fulfilling these conditions is called Hermitian. All geophysical spectra are Hermitian. Furthermore, since

$$F(\omega) = a(\omega) + i b(\omega) = |F(\omega)| e^{i\phi(\omega)}$$

then the modulus $F(\omega)$ is even and the phase $\phi(\omega)$ is odd.

The time-shifting theorem is also a useful property. Given that $f(t)$ transforms to $F(\omega)$, then for a real constant alpha (α),

$$f(t \pm \alpha) \rightarrow e^{\pm i\alpha\omega} F(\omega) = |F(\omega)| e^{i(\phi\omega) \pm i\alpha\omega}.$$

If a time function is shifted by a constant amount, then its amplitude spectrum remains unchanged while its phase spectrum changes by a linear amount determined by the time shift. This property is useful to control the position of the final time domain filter in the transform window.

EXPERIMENTAL PROCEDURE

An experiment was designed that would test the phase response of the playback electronics within the seismic bandwidth 2 to 25 hertz. The test signal was the clock's internal 2 kilohertz oscillator that was divided down by 1024 to produce an accurate, stable square wave of frequency 1.9531250 hertz. The number of sample points used in the Fast Fourier Transform (FFT) routine was 1024. This assured a whole number of cycles, 20, in the sample window. The frequencies present in a square wave are the fundamental plus an exponentially decreasing series of the odd harmonics. Thus, the frequencies sampled using this square wave are approximately 2, 6, 10... hertz. The test signal was inserted at the record head amplifier of all three channels but by-passed the other active electronics of the OBS. The clock signal was recorded to synchronize the digitization on playback.

COMPUTATION OF THE FILTER

The filter is constructed in the frequency domain utilizing only the fundamental and odd harmonic frequencies. The algebra of the filter is as follows. One can define the principal time functions as:

$s(t)$ =input square wave
 $d(t)$ =distorted output
 $f(t)$ =inverse filter
 $g(t)$ =forward filter.

and in frequency space each time function Fourier transforms to,

$s(t)$ becomes $S(w)$
 $d(t)$ becomes $D(w)$
 $f(t)$ becomes $F(w)$.

Simple filter theory states that an input is convolved (*) with a filter to produce an output (equation 1).

$$s(t)*g(t)=d(t) \quad (1)$$

An inverse filter, $f(t)$, can be found such that

$$g(t)*f(t)=\delta(t),$$

the unit spike function. Convoluting $f(t)$ with equation 1 produces

$$s(t)*g(t)*f(t)=d(t)*f(t).$$

Since a function convolved with a delta function is the original function, then

$$s(t)=d(t)*f(t). \quad (2)$$

If a suitable filter can be constructed, then the original signal is recovered by convolving $f(t)$ with the distorted output.

Convolution in one domain is equal to multiplication in the transform domain. Thus equation 2 can be directly written in Fourier space as,

$$\begin{aligned} S(w) &= D(w) \cdot F(w) \\ \text{or} \\ F(w) &= S(w)/D(w). \end{aligned} \quad (3)$$

The functions $S(w)$, $D(w)$, and $F(w)$ are complex (equation 4) so that the filter $F(w)$ can be expressed as a complex division (equation 5).

$$\begin{aligned} S(w) &= X_s + iY_s \\ D(w) &= X_d + iY_d \end{aligned} \quad (4)$$

$$F(w) = \left[\frac{X_s \cdot X_d + Y_s \cdot Y_d}{X_d^2 + Y_d^2} \right] + i \left[\frac{Y_s \cdot X_d - Y_d \cdot X_s}{X_d^2 + Y_d^2} \right] \quad (5)$$

The frequencies present in the test square wave are the odd harmonics of 1.953251 hertz. These frequencies are identical to the discrete Fourier frequencies calculated for 1024 points by the FFT program. Thus only the complex values at the harmonics are used in equation 5 to calculate the complex values of the filter.

The filter is also Hermitian and must satisfy the oddness/evenness properties in a smooth fashion. Figure 5 displays two partial plots of the imaginary values of the filter, near the edges of the frequency window where the amplitude of the imaginary part must go through zero. The circles are the discrete frequency values and the connecting line was calculated using a cubic spline interpolation routine. However, two alterations were made in generating the continuous version. First, a Gaussian curve was applied from 0 to 6 hertz with the 1.95 hertz value eliminated. This produced a smooth transition to zero hertz and prevented the filter from trying to compensate for the natural low frequency rolloff of the playback head. At the folding point or Nyquist frequency, the oddness requirement was satisfied by eliminating the 48.8 hertz value and by a similar Gaussian smoothing from 45 to 50 hertz. The real part of the filter was cubic spline interpolated between harmonic values with a smooth continuation to the folding point (figure 6).

The functions $S(w)$ and $D(w)$ can be alternatively expressed as Fourier series (equation 6).

$$S(w) \sim S_w = \sum_n S_n e^{i(\omega_n t + \theta_n^s)} \\ D(w) \sim D_w = \sum_n D_n e^{i(\omega_n t + \theta_n^d)} \quad (6)$$

The expression for the filter in equation 3 becomes,

$$F(w) \sim F_w = \sum_n \left(\frac{S_n}{D_n} \right) e^{i(\theta_n^s - \theta_n^d)}$$

The response of the filter is the ratio of the amplitude responses, S_n and D_n , and the difference in the phase responses. The amplitudes at the harmonics are practically equal (figure 7), and the ratio (S_n/D_n) is approximately unity. In other words, the filter does not alter the Fourier amplitudes in the signal significantly.

The phase response of a perfect square wave is a constant. However, an initial time shift will result in a linear slope in the phases. This slope is seen in the phase responses of S_w and D_w (figure 8). The difference in these phases (lower plot) is the response of the filter but with a different slope. The deviation from this slope is the phase angle correction that is applied to the signal. The phase distortion occurs in the seismic bandwidth 2 to 15 hertz (figure 8) and is most severe below 10 hertz.

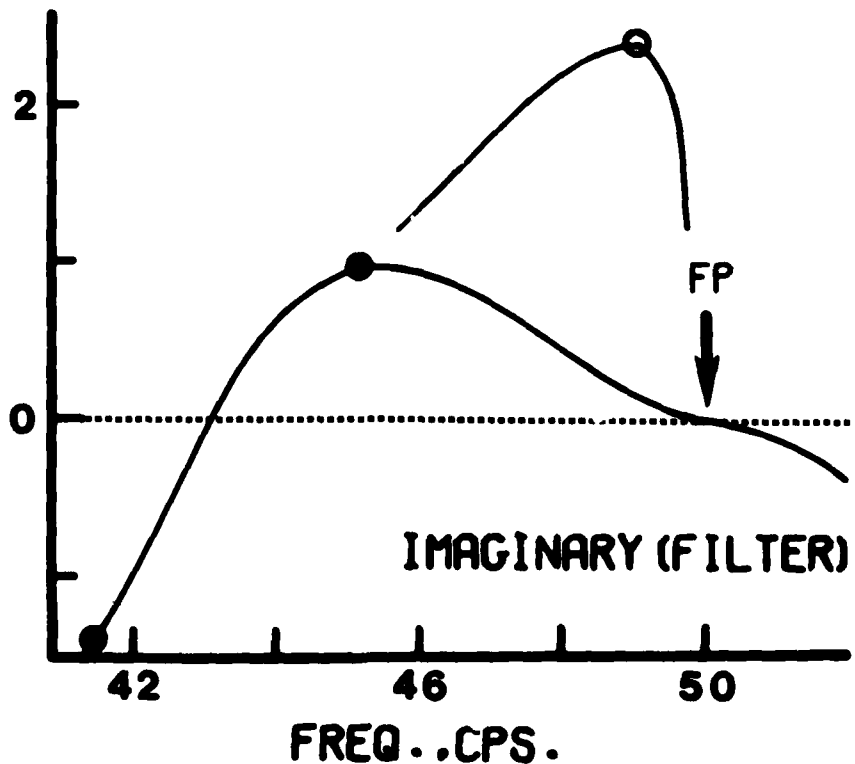
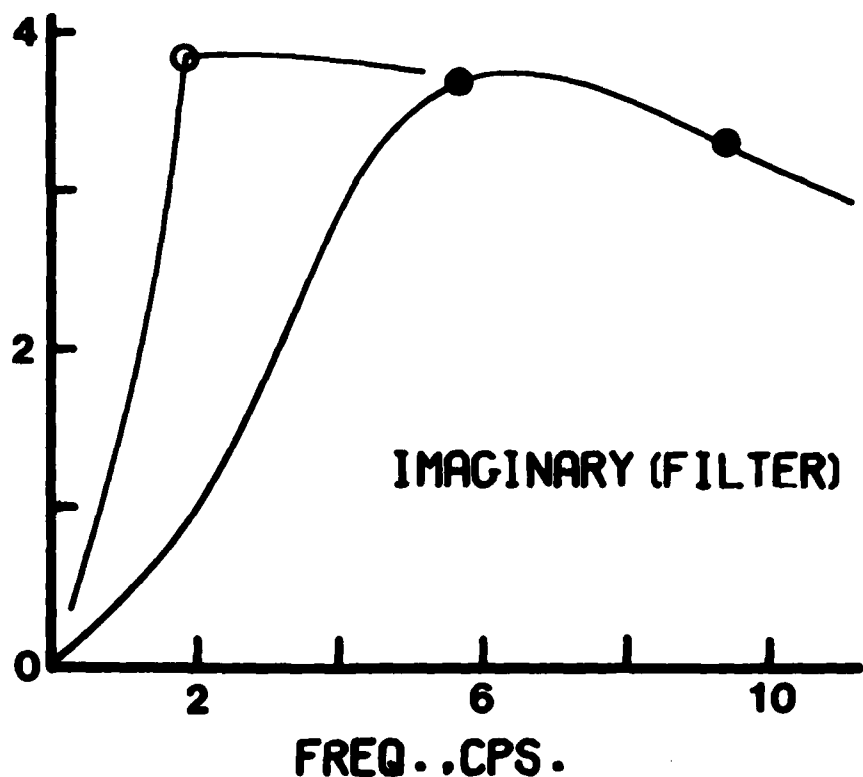


FIGURE 5. Plots of the imaginary part of the complex inverse filter. Ordinate units are arbitrary. See text for discussion.

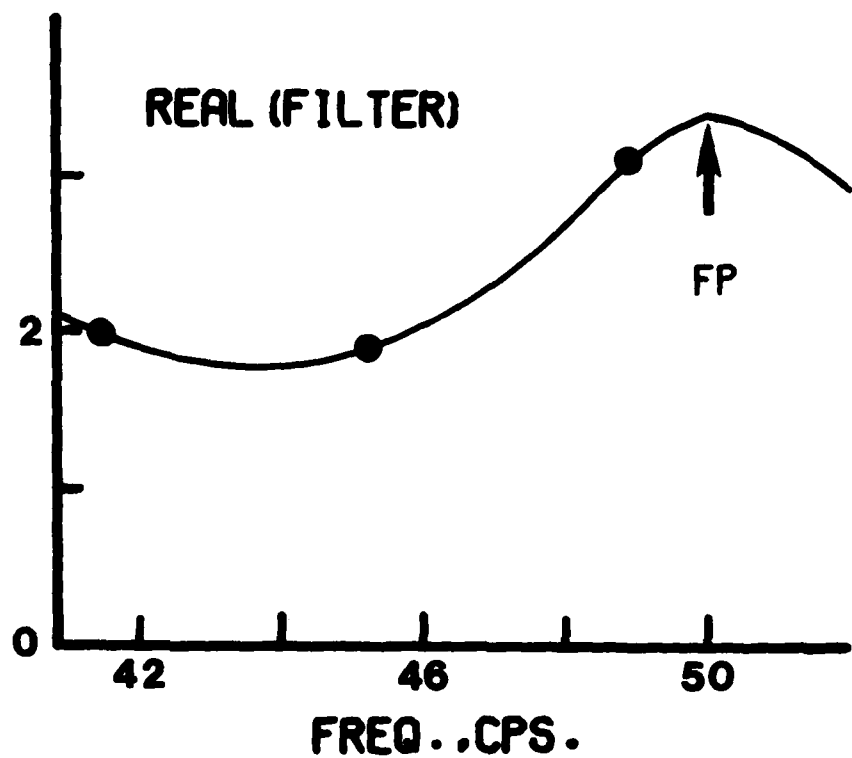
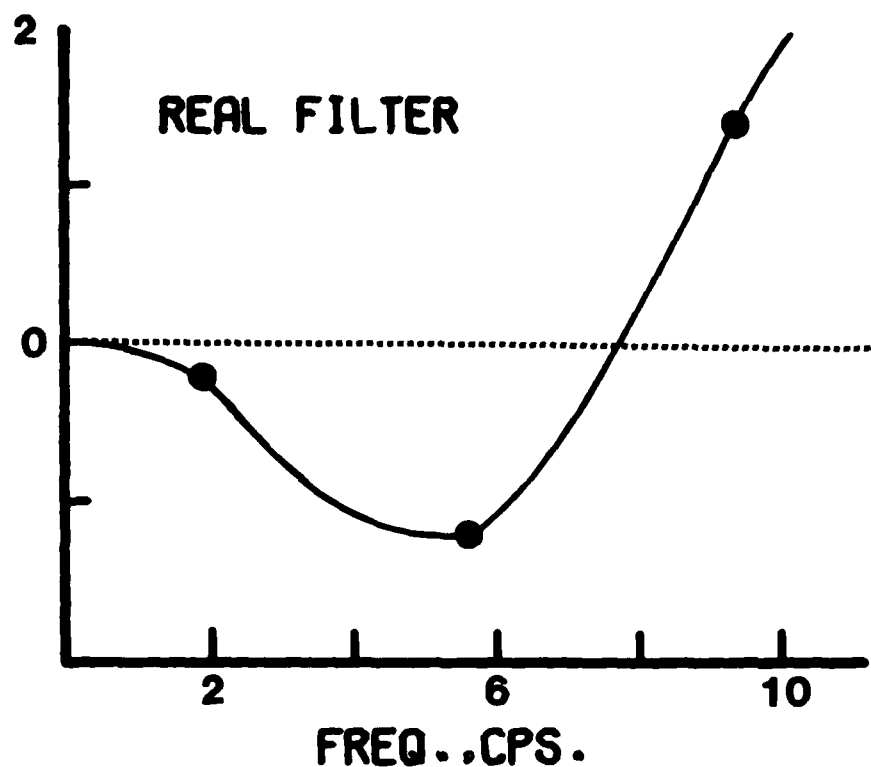


FIGURE 6 Plots of the real part of the complex inverse filter, near the edges of the frequency window.

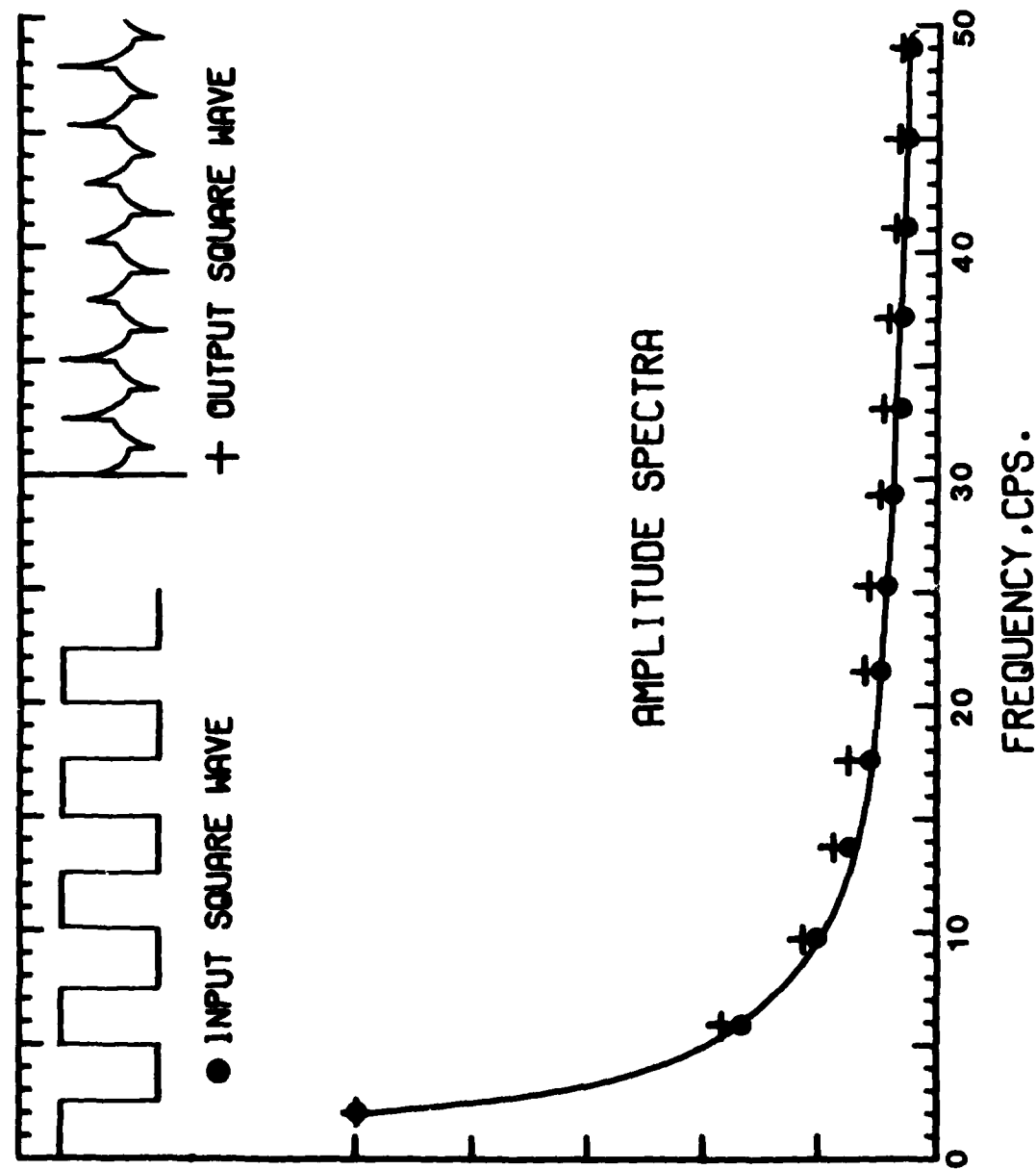


FIGURE 7. A comparison of the amplitude spectra of a perfect square wave (filled circles) with the spectra of the distorted output (crosses). The amplitude scale is linear and the plots have been normalized to 1.

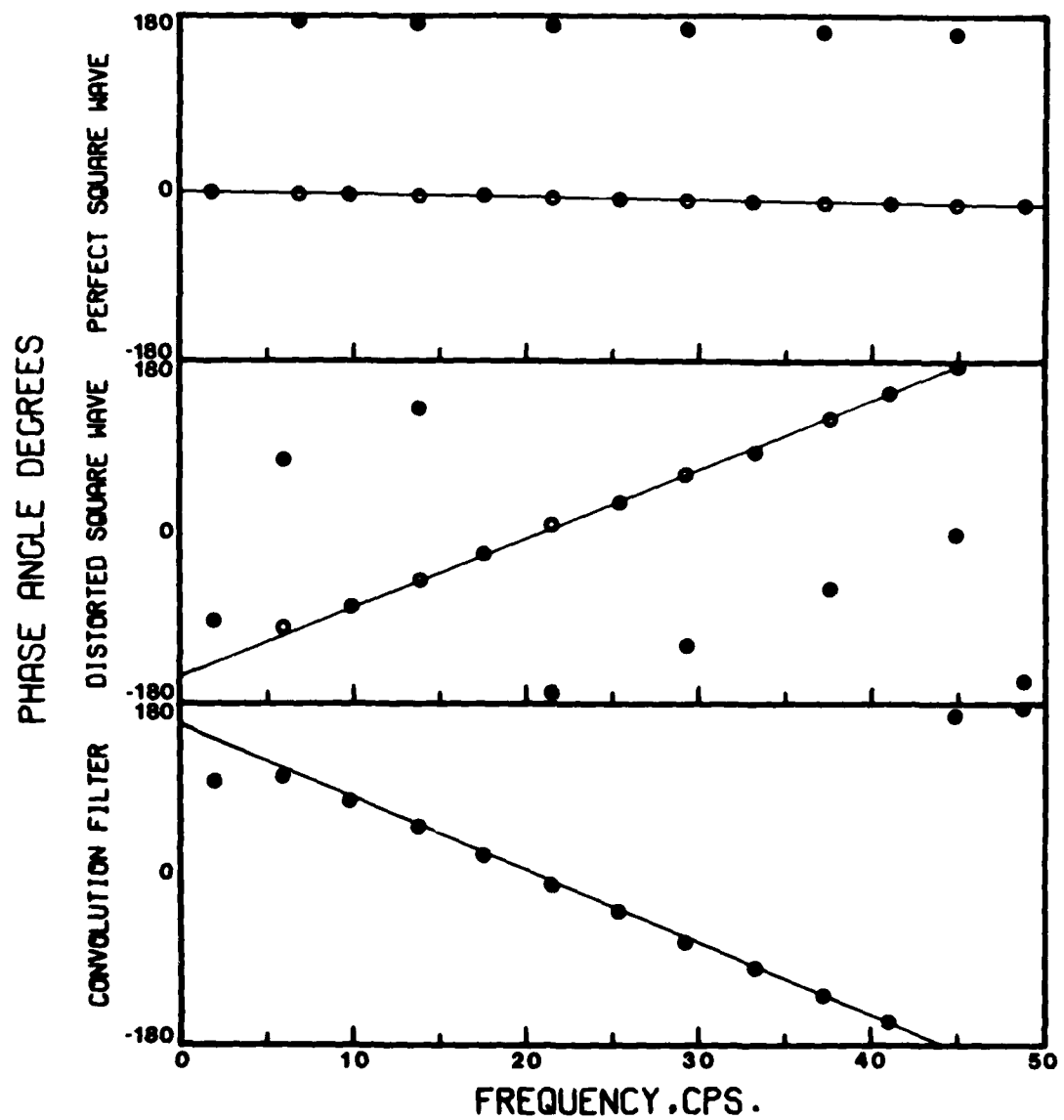


FIGURE B. A comparison of the phase responses of a perfect square wave, the distorted output signal, and the final inverse phase filter over the bandwidth 0 to 50 hertz.
EXPLAIN DOTS AND CIRCLES

TIME DOMAIN REPRESENTATION OF THE FILTER

The phase-correcting filter was constructed and modified in the frequency domain. It is inverted to a time domain function by an inverse Fourier transform and consists of 1024 points, the same number as in the frequency domain. Figure 9 is a plot of the middle 250 points of the filter. The energy is limited to the center points with the tails being near zero. The filter's amplitude spectrum can be regarded as flat, even on this exaggerated linear scale (figure 9). The center 50 points (0.5 seconds) of the filter retains greater than 99 percent of the total power of the original filter. This length filter can be effectively convolved with the signal to produce the desired results. In addition, the resultant 50 point operator is computationally efficient for moderate length data sets.

The final truncated filter is smoothed by a running 3-point binomial filter. This has the desired effect of low-pass filtering the inverse filter to remove any residual high frequency oscillations. However, the filter remains flat over the seismic bandwidth 5 to 20 hertz, and the response is minus 3db in amplitude at 3 and 22 hertz with a slow roll-off to the Nyquist frequency, 50 hertz.

RESULTS

A test of the filter was made by convolving the truncated version with the original distorted square wave. Figure 10 is a sketch of several cycles of the filtered square wave. The phase correction has been accomplished effectively. A very slight rounding and overshoot is present on the square wave edges due to the steps taken to smooth the filter, but the anomalies are smaller than the random variations due to tape and head-amplifier noise.

The final result obtained by convolving the phase correction filter with a seismic trace is displayed in figure 11 (trace PHASE). The initial trace, labeled RAW, is the digitized, square-rooted signal. The SQR-trace is the result of bi-polar squaring the RAW-signal. The waveform is overall spiky in nature and the first-energy arrival time is a half-cycle late, about 0.03 seconds. Additional traces

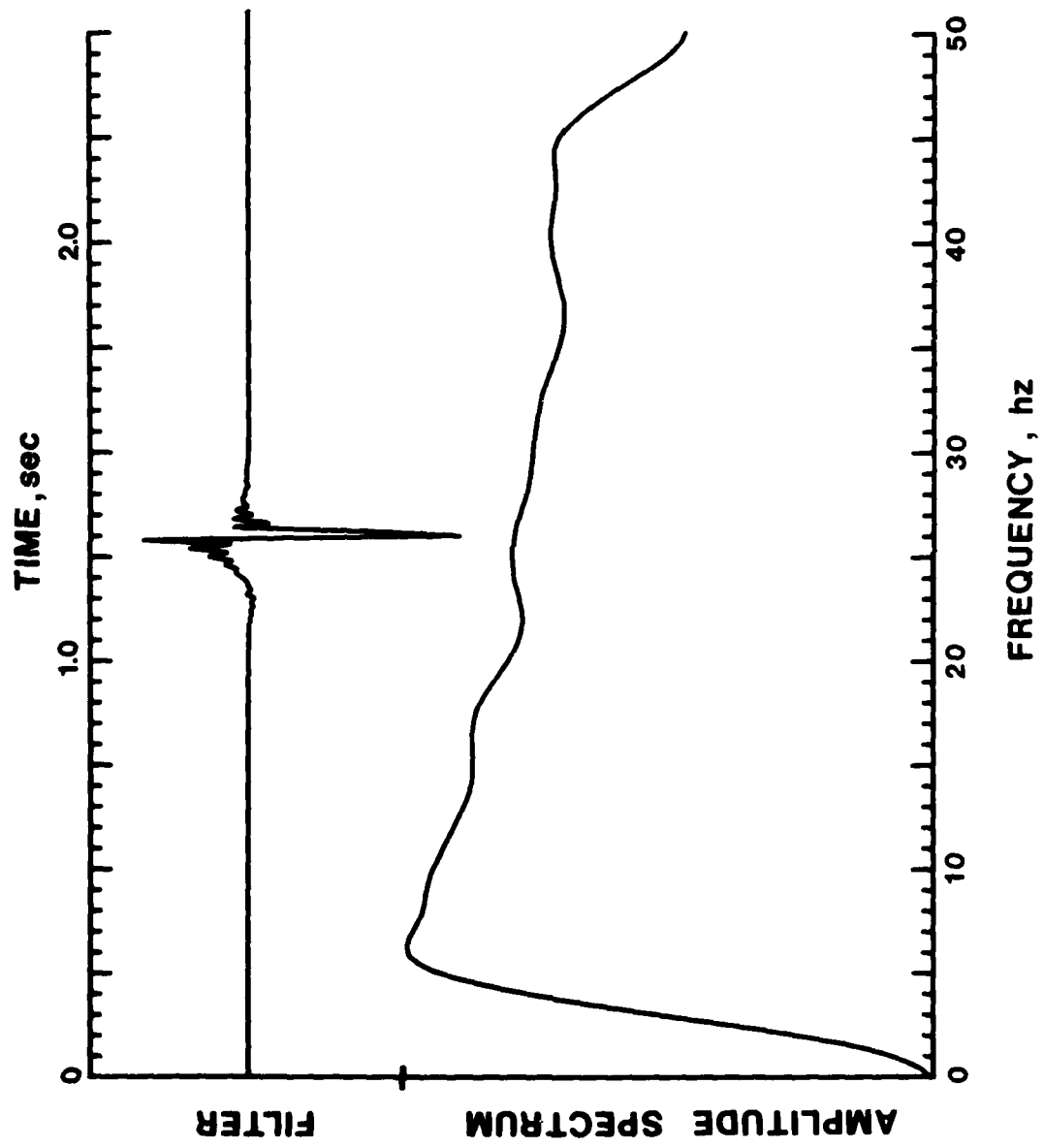
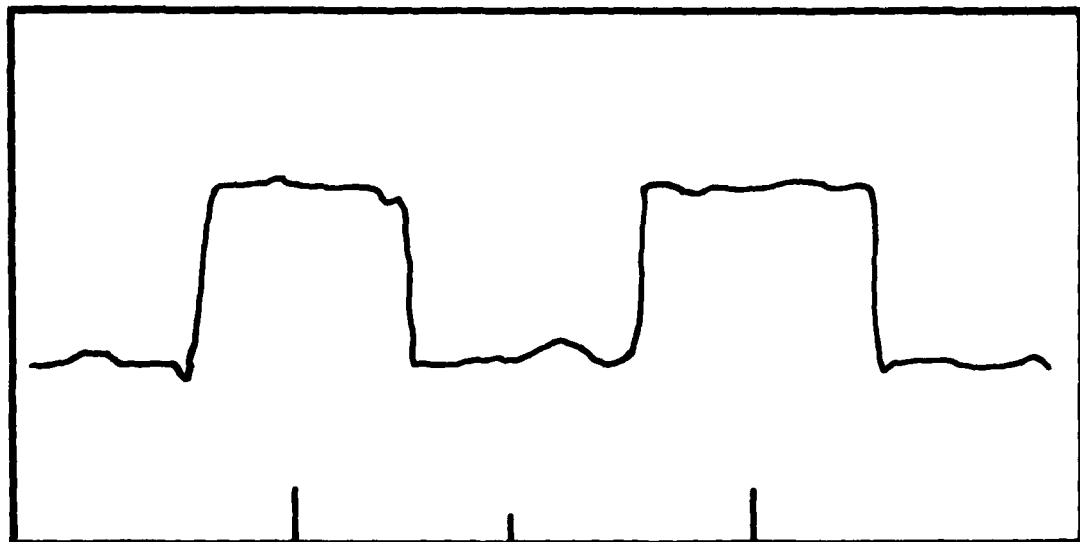


FIGURE 9. A linear plot of the amplitude spectra of the inverse phase filter



0.5 sec.

FIGURE 10. A sketch of the waveform that results from convolving the distorted square wave signal with the inverse phase filter.

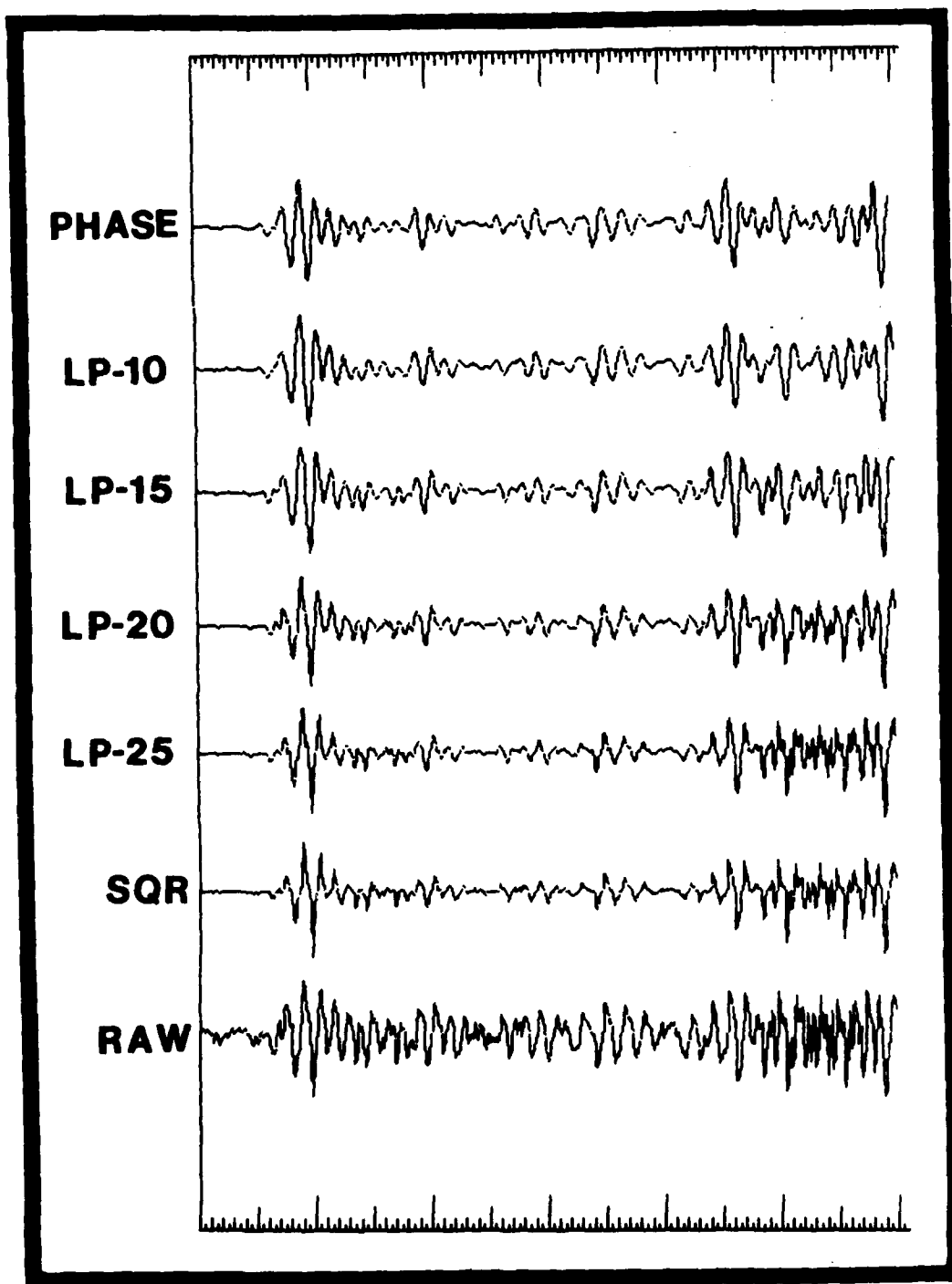


FIGURE 11. A comparison between the RAW seismic signal and the phase corrected signal, trace PHASE. The SQR-trace is the raw signal squared, and the LP-traces are various low-pass filtered signals. Refer to text for discussion.

were generated from the raw squared data by progressively filtering out more and more of the high frequencies, consisting mostly, but not exclusively, of spurious harmonics of the basic seismic signal. They are designated LP- and the -3db cutoff point in hertz of a zero-phase shift low-pass convolution filter less than 0.5 seconds in length. The difference between these LP-signals and trace-PHASE are subtle but significant. The general waveform progresses from being very spiky (LP-25) to being overly 'filtered' looking (LP-10). The first motion of the PHASE-trace is a distinct positive (upward) pulse. Only trace LP-10 begins to show the first arrival properly, but it is still several hundredths of a second late. It should be noted that the amplitudes for each trace are relative to a maximum excursion of one inch, and therefore can not be used for direct comparison. However, the amplitude of the first arrival wave packet of the LP-traces were usually no more than 80 percent of that of the PHASE-trace.

CONCLUSIONS

Until recently nearly all the results obtained from marine seismic refraction have been based on the analysis of the travel-time distance relations for the most prominent arrivals on the records. In this report, and its companion (Determination of the orientation and gain of horizontal geophones used in ocean bottom seismometers, Technical Report Number 386) new methods have been described which attempt to obtain a more detailed model of the velocity structure by making use of more of the information on the seismograms. The combinations of travel-time analysis with studies of the true amplitudes, particle motions and waveforms of the arrivals, places much greater constraints on the velocity structure and increases the potential resolution of the refraction technique. In the future, the spectral content of an arrival may be as valuable in deducing detailed structure as the timing of that arrival, or its raw amplitude. To obtain this information, it is essential that the characteristics of the receiver and playback electronics be well known and corrected for in processing as well as practicable.

The unprocessed signal from the University of Washington OBS showed that some form of distortion was occurring in the seismic bandwidth. By recording a synchronised square wave, and comparing the output with the input in the frequency domain, it became obvious that the lower harmonics of the square wave were being phase shifted. A phase correcting filter was constructed in the frequency domain and inverted to a time domain convolution operator of 50 points (0.5 second) length.

REFERENCES

Johnson, R. V., C. R. B. Lister, and B. T. R. Lewis. A direct recording ocean bottom seismometer. *Marine Geophysical Researches*, 3, 65-85, 1977.

Lister, C. R. B. and B. T. R. Lewis. An ocean bottom seismometer suitable for arrays. *Deep Sea Research*, 23, 113-124, 1976.

FOR UNCLASSIFIED TECHNICAL REPORTS, REPRINTS & FINAL REPORTS
PUBLISHED BY OCEANOGRAPHIC CONTRACTORS
OF THE OCEAN SCIENCE & TECHNOLOGY DIVISION
OF THE OFFICE OF NAVAL RESEARCH

12 Defense Documentation Center
Cameron Station
Alexandria, Virginia 22314

Office of Naval Research
Department of the Navy
Arlington, Virginia 22217

6 ATTN: Code 102-IP

1 Cognizant ONR Branch Office
1030 East Green Street
Pasadena, California 91106

1 ONR Resident Representative

Director
Naval Research Laboratory
Washington, D.C. 20375

6 ATTN: Library, Code 2627

Scientific Officer
NORDA
Bay St. Louis, Mississippi 39520

1 ATTN. Code 461

Unclassified

SECURITY CLASSIFICATION OF THIS PAGE (When Data Entered)

REPORT DOCUMENTATION PAGE		READ INSTRUCTIONS BEFORE COMPLETING FORM
1. REPORT NUMBER	2. GOVT ACCESSION NO.	3. RECIPIENT'S CATALOG NUMBER
Technical Report No. 385	AD-A216 303	
4. TITLE (and Subtitle)	5. TYPE OF REPORT & PERIOD COVERED	
A phase correction filter for waveform recovery of compressed direct-recorded ocean bottom seismometer data.	Final 1975-1978	
6. AUTHOR(s)	7. PERFORMING ORG. REPORT NUMBER	
Ules S. Wade and Clive R.R. Lister	M81-06	
8. CONTRACT OR GRANT NUMBER(s)	N-00014-75-C-0502	
		MOD P00021
9. PERFORMING ORGANIZATION NAME AND ADDRESS	10. PROGRAM ELEMENT, PROJECT, TASK AREA & WORK UNIT NUMBERS	
University of Washington Department of Oceanography Seattle, Washington 98195	Project NR 083-012	
11. CONTROLLING OFFICE NAME AND ADDRESS	12. REPORT DATE	
Office of Naval Research La Jolla, California	March 1981	
13. NUMBER OF PAGES	14. MONITORING AGENCY NAME & ADDRESS (if different from Controlling Office)	
21	15. SECURITY CLASS. (of this report)	
		Unclassified
		16. DECLASSIFICATION/DOWNGRADING SCHEDULE
17. DISTRIBUTION STATEMENT (of the abstract entered in Block 20, if different from Report)		
Approved for public release: distribution unlimited.		
18. SUPPLEMENTARY NOTES		
19. KEY WORDS (Continue on reverse side if necessary and identify by block number)		
Marine geophysics Thomas G. Thompson cruises Ocean bottom seismometer Marine seismic refraction profiles Phase correction digital processing		
20. ABSTRACT (Continue on reverse side if necessary and identify by block number)		
A phase correction convolution filter has been developed for the University of Washington's ocean bottom seismometers to correct severe waveform distortion on playback. Signals are recorded directly on magnetic tape after compression by taking the bipolar square-root of the signal. Prior to digitization, the analog playback head shifts the phases of the low frequency and thus distorts the recorded waveform. If the distorted signal is squared without correction, the original waveforms and bandwidths are not recovered, leading to errors in the analysis of the seismic data.		

DAT
ILM